Proc. Int. Symposium on Neutron Optics and Related Research Facilities, Kumatori, 1996
J. Phys. Soc. Jpn. **65** (1996) Suppl. A pp. 271-276

New Aspects of Dynamical Diffraction Phenomena of Neutrons

Toshio Takahashi

Institute for Solid State Physics, University of Tokyo, Roppongi, Minato-ku, Tokyo 106, JAPAN

(Received 18 February 1996; accepted 5 May 1996)

Theoretical and experimental studies of dynamical diffraction phenomena of neutrons and X-rays by single crystals have been made from new points of view. Based on the dynamical diffraction theory we have developed, new properties of the rocking curve and the Fresnel reflectivity curve are explained. The rocking curve in the symmetric Bragg-case has a possibility to give a precise value of scattering amplitudes when it is given as a function of perpendicular momentum transfer. It is shown that the Fresnel reflectivity curve is identical to the Darwin curve with an appropriate transformation. It is also shown that in the case of non-absorbing thick crystals the Ewald formula can be obtained by summing up the intensity of incoherent beams successively reflected at the front and rear surfaces. This interpretation gives a simple relation of the Ewald formula to the Darwin formula. A double Stern-Gerlach experiment is proposed by using a new type of crystal interferometer.

KEYWORDS: dynamical theory, rocking curve, reflectivity, Darwin curve, Ewald curve, neutrons, X-rays, double Stern-Gerlach

§.1. Introduction

Diffraction and scattering phenomena of neutrons and X-rays have been used for studying the structure of materials. The measurement of rocking curves has been used to study the structure of crystals, superlattices, mirrors and so on.[1-3] The Fresnel reflectivity curve near the critical angle of total reflection gives information on the perpendicular structure near the surface of various kinds of materials.[4-7] It has been found that CTR(Crystal Truncation Rod) scattering is sensitive to the structure of crystal surfaces.[8-10] Hitherto, different theoretical approaches have been used to analyze those kinds of data.

Recently we have developed a dynamical theory of X-ray diffraction[11,12] which is applicable to Bragg diffraction, Fresnel reflectivity, and CTR scattering. The theory has been constructed on the basis of the Darwin theory in a matrix form,[13-15] and the results can be easily applied to the neutron cases.

In this paper, first we show some properties of the rocking curve and the Fresnel reflectivity curve based on the theory we have developed. Next we show results on measurements of neutron rocking curves by perfect silicon crystals, and show a new interpretation of the diffraction process. Finally, we propose an experiment on measurement theory in quantum mechanics using an LLL interferometer.

§.2. Extended Darwin Theory

In the Darwin theory,[13] a crystal is divided into layers parallel to the crystal surface, and the effect of multiple reflection between the layers is taken into the difference equations. Therefore the Darwin theory is suited for treating the diffracted intensities from a substance with a layered structure and a crystal with a different structure on its surface. For this reason, the Darwin theory has attracted renewed interests in combination with a matrix method.[14]

We have combined the Darwin theory with the idea of the reciprocal rod, that is, the truncation rod. As a result of this, we have succeeded in deriving expressions which can give the diffracted intensities along the rod from Bragg point to Bragg point even in the case of asymmetric geometry.[12]

One of the great differences from the conventional theory[16-21] is that one needs the direction of the diffracted beam θ_H for a given incidence direction θ_0 to obtain the diffracted intensity. This point can be solved if one notices that the measurement of the rocking curve near the Bragg point corresponds to the intensity variation along the reciprocal rod elongated from the Bragg point not only in the symmetric case but also in the asymmetric case.

2.1 General Expression for the Bragg-Case

Once one knows the direction of the exit beam for a given incidence condition, one can calculate the reflection and transmission coefficients by a single atomic layer. Then one can solve the difference equations using the matrix method.

In this paper, we discuss only the result on a perfect crystal. Here we show the result on the reflection coefficient from a semi-infinite crystal in the Bragg-case. A general expression of the reflection coefficient $R_{H,\infty}$ is given by

$$R_{H,\infty} = -|b|^{1/2}\frac{C}{|C|}\frac{F_H}{[F_h F_{\overline{H}}\exp(-i2\pi l)]^{1/2}}[\eta \mp (\eta^2-1)^{1/2}] \tag{2.1}$$

using a deviation parameter η defined by

$$\eta = \frac{i\dfrac{\lambda}{2\pi d}\gamma_0\exp(i2\pi l)+\dfrac{1}{2}F_0(1-b)}{|C||b|^{1/2}\,\Gamma[F_H F_{\overline{H}}\exp(-i2\pi l)]^{1/2}} \tag{2.2}$$

with

$$\Gamma = \frac{r_e\lambda^2}{\pi V}. \tag{2.3}$$

Here λ is the wavelength, d is the distance between the layers, and r_e is the classical electron radius for X-rays and one for neutrons. The polarization factor C in the case of X-rays is one for neutrons. The asymmetric factor b is defined by $b = \gamma_0/\gamma_H$ using direction cosines of the incident beam $\gamma_0 = \cos\theta_0$ and the diffracted beam $\gamma_H = \cos\theta_H$. V is the volume of the unit cell. It is noted that the unit cell of the crystal is always defined to be parallel to the surface.

The index H represents the indices hkl; the indices h and k designate the reciprocal rod arising from the two-dimensional periodicity of the layer and take the value of integers, and the index l denotes a point on the hk rod. The value of the index l coincides with an integer at the kinematical Bragg condition, but does not necessarily take the value of integer. Thus the structure factor F_H is calculated for the point l on the hk rod.

The index l corresponds to a perpendicular momentum transfer normalized by the reciprocal vector perpendicular to the crystal surface a_3^*, and is given by

$$l = \frac{\cos\theta_0 - \cos\theta_H}{\lambda|a_3^*|}. \qquad (2.4)$$

In this theory, effect of the surface structure on the intensity is easily taken into account as the products of matrices characterizing each surface layer.

2.2 Relationship With the Conventional Diffraction Theory

Since the index l takes the value of integer at a Bragg point, $\exp(i2\pi\, l)$ is approximated to $1 + i2\pi\,(l - l_{\mathrm{int}})$ near the Bragg point denoted by $l = l_{\mathrm{int}}$. Then the deviation parameter η given by eq.(2.2) is approximated to

$$\eta = \frac{-\gamma_0(\gamma_0 - \gamma_H - \dfrac{\lambda}{d} l_{\mathrm{int}}) + \dfrac{1}{2}F_0(1-b)}{|C||b|^{1/2}\,\Gamma[F_H F_{\bar{H}}]^{1/2}}, \qquad (2.5)$$

and the reflection coefficient is given by

$$R_{H,\infty} = -|b|^{1/2}\frac{C}{|C|}\frac{F_H}{[F_h F_{\bar{H}}]^{1/2}}[\eta \mp (\eta^2 - 1)^{1/2}], \qquad (2.6)$$

since $\exp(i2\pi\, l) \cong 1$.

One can easily obtain the well-known deviation parameter[18)]

$$\eta = \frac{-b\sin 2\theta_B \Delta\theta_0 + \dfrac{1}{2}F_0(1-b)}{|C||b|^{1/2}\,\Gamma[F_H F_{\bar{H}}]^{1/2}} \qquad (2.7)$$

by expanding eq.(2.5) around the kinematical Bragg angle θ_B up to the first order term on $\Delta\theta_0 = \theta_0 - \theta_B$.

2.3 Specular Reflection

The expression of the reflection coefficient given by eq.(2.1) is valid for any incidence condition. Figure 1 shows the reflectivities of neutrons and σ-polarized X-rays with a wavelength of 1.0 Å as a function of the index l calculated from eq.(2.1) for the 00 rod of the Si(111) surface terminated by the unreconstructed double-layer. The peaks mean the Bragg reflections, and their tails correspond to the CTR scattering.

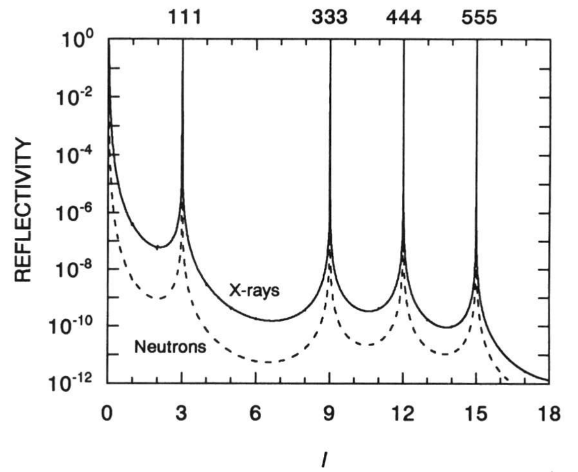

Fig.1. Reflectivities of neutrons and σ-polarized X-rays as a function of l, calculated by eq.(2.1) along the 00 rod, for the Si(111) crystal terminated by the ideal double-layer.

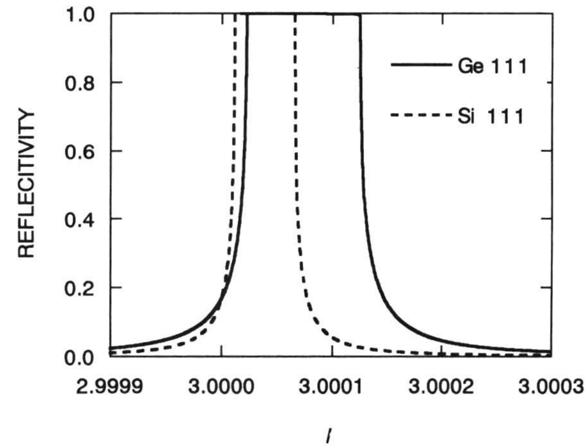

Fig.2. Neutron rocking curves in l-scale for 111 reflections of Si and Ge.

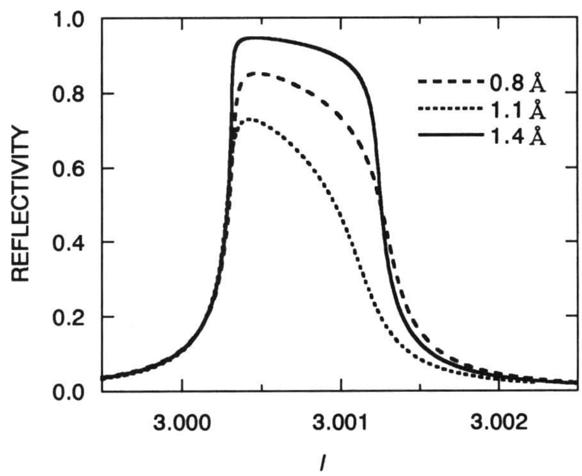

Fig.3. Effect of anomalous scattering on the X-ray rocking curve of Ge 111 reflections in l-scale.

From eq.(2.2), one can show that the reflectivity curve in l-scale is independent on the wavelength in the case of symmetric geometry, that is, $\gamma_0 = |\gamma_H|$, neglecting the effect of anomalous scattering in the case of X-rays. This indicates that the rocking curve near the Bragg point as a function of l, instead of η or θ_0, reflects more directly the scattering lengths of atoms.

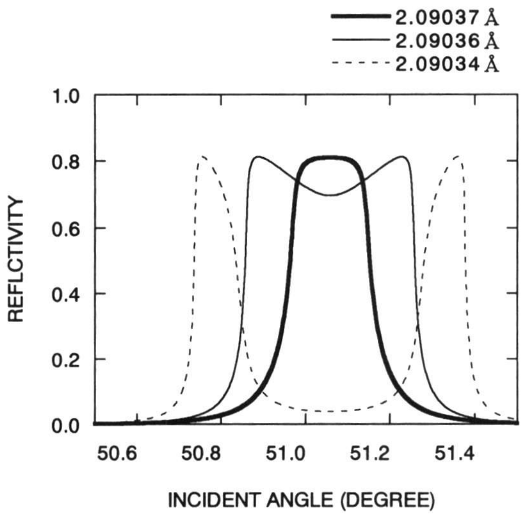

Fig. 4. X-ray rocking curves as a function of incident angle θ_0 satisfying the condition of $\theta_B \cong 90°$.

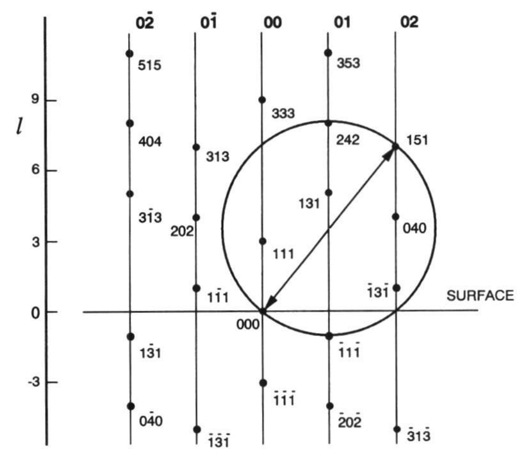

Fig. 5. Ewald construction in the case of $\theta_B \cong 90°$.

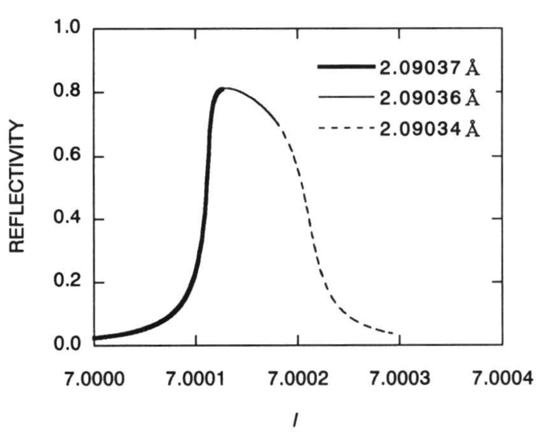

Fig. 6. X-ray rocking curves in l-scale corresponding to those in Fig. 4.

Figure 2 shows the calculated neutron rocking curves near the 111 Bragg point of Si(111) and Ge(111) crystals as a function of l. The value of l which gives the center of the Bragg peak shifts slightly from the integer due to the refraction effect. The difference in width between the Darwin curves of Si and Ge is due to that in value between the nuclear scattering lengths. Therefore precise measurements of the rocking curve in l-scale have the possibility of giving the value of the magnetic scattering amplitudes in the case of neutron diffraction and the anomalous scattering amplitudes in the case of X-ray diffraction.

Figure 3 simulates the rocking curves in l-scale for Ge 111 reflections of X-rays with wavelengths around the K-absorption edge: 0.8Å, 1.1Å and 1.4Å. The difference of profiles reflects that of anomalous scattering factors.

2.4. Bragg Condition of $\theta_B \cong 90°$

Diffraction phenomena of the Bragg condition of $\theta_B \cong 90°$ have been studied extensively in the conventional theory because the Darwin width increases remarkably as the Bragg angle approaches to 90°.[22-24] In X-ray standing wave method,[25,26] this nature is utilized to apply the method to wide variety of samples.

In this geometry, however, the conventional theory requires special treatment of the dispersion surface. In the present theory, however, one can deal with such diffraction condition without special treatment by using eq.(2.5).

One of the features on this condition is that anomalous changes in the rocking curve appear in angle-scan mode but disappear in wavelength-scan mode. Figure 4 demonstrates an example of such rocking curves of 511 reflections in the case of X-rays: thick solid line for 2.09037 Å, solid line for 2.09036 Å, and broken line for 2.09034 Å. This fact is easily understood if one describes the diffraction condition by the intersection of the Ewald sphere with the rod as shown in Fig. 5. The rocking curves in l-scale are shown in Fig. 6. In this scale, all the curves coincides among themselves because $\gamma_0 = |\gamma_H|$ even in the case of asymmetric geometry illustrated in Fig. 6.

Another feature is that the Darwin width ω on this condition is proportional to

$$\omega \cong \sqrt{2\Gamma|F_H|} \tag{2.8}$$

while that in the ordinary condition is proportional to $\Gamma|F_H|$. This is understood from a point that the approximation given by eq.(2.7) fails when $\sin 2\theta_B$ approaches to zero. The deviation parameter in this condition should be approximated to

$$\begin{aligned}\eta = [&-b\sin 2\theta_B \Delta\theta_0 \\ &+\frac{1}{2}(2\sin 2\theta_B - b\cos 2\theta_B + b^3)(\Delta\theta_0)^2 \\ &+\frac{1}{2}F_0(1-b)] \times \frac{1}{|C||b|^{1/2}\,\Gamma[F_H F_{\bar{H}}]^{1/2}}\end{aligned} \tag{2.9}$$

by expanding eq.(2.5) up to the second order of $\Delta\theta_0$. From this equation, one can show that the Darwin width in this condition is given by the relation of eq.(2.8).

2.5. Fresnel Reflectivity

In the Darwin theory, the transmission and reflection coefficients from a single layer diverge at an extreme grazing incidence condition. Therefore, strictly speaking, the present theory breaks in the region of total reflection.

If, however, we start from the relation given by eq.(2.5), we can extract the Fresnel formula as follows.

The deviation parameter η is expressed as

$$\eta = -\frac{\cos^2\theta_0 - \delta}{\delta} \quad , \qquad (2.10)$$

assuming that $F_H = F_{\bar{H}} = F_0$ in eq.(2.5). Here δ is defined by

$$\delta = \frac{1}{2}\Gamma F_0 \ , \qquad (2.11)$$

and related to the refractive index n by

$$n^2 = 1 - 2\delta \ . \qquad (2.12)$$

Then the reflection coefficient is given by

$$R_{H,\infty} = -[\eta \mp (\eta^2 - 1)^{1/2}] \qquad (2.13)$$

$$= \frac{\cos\theta_0 - \sqrt{n^2 - \sin^2\theta_0}}{\cos\theta_0 + \sqrt{n^2 - \sin^2\theta_0}} \ . \qquad (2.14)$$

This means that the Fresnel reflectivity curve has the same profile as the Darwin curve in η-scale. The critical angle of total reflection corresponds to the condition of η = -1, that is, $\cos^2\theta_0 = 2\delta$. If we interpret the total reflection as a special case of Bragg diffraction, there is some resemblance between total reflection and Bragg reflection of $\theta_B = 90°$ because the condition of $\sin 2\theta_B = 0$ is satisfied. In this situation, the region of total reflection ω, that is, the critical angle, is proportional to

$$\omega \cong \sqrt{\Gamma F_0} \qquad (2.15)$$

Fig. 7 shows the total reflection curve together with the field intensity at the surface as a function of $\eta' = \mathbf{Re}(\eta)$.

In the case of neutrons, the reflectivity curve is usually given as a function of perpendicular momentum transfer because the curve in this representation is independent on the wavelength. This fact is consistent with the result given in section 2.3.

§.3. Interpretation of the Ewald Curve

Diffraction phenomena of neutrons by a perfect crystal are explained by the dynamical theory.[20,21] The diffracted intensity of neutrons from non-absorbing crystals in the Bragg-case is usually explained by the Ewald formula[27] expressed as

$$I_H^{(E)} = \begin{cases} 1 & \text{for } |\eta| \le 1 \\ 1 - (1 - \eta^{-2})^{1/2} & \text{for } |\eta| \ge 1 \end{cases} \qquad (3.1)$$

Here η is given by the deviation parameter indicated by eq.(2.7). Total reflection occurs in the region of $|\eta| \le 1$.

In contrast, the diffracted intensity of the Darwin curve in the case of symmetric diffraction is given by

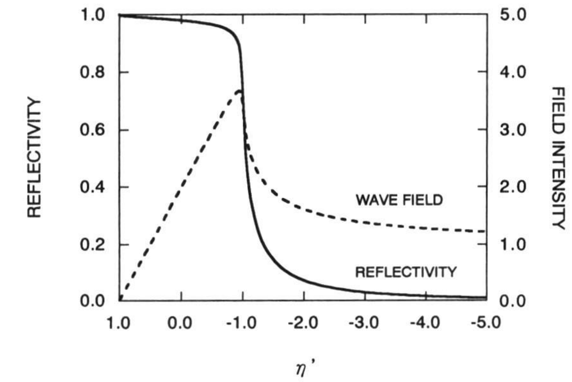

Fig. 7. X-ray Fresnel reflectivity curve in η-scale and field intensity at the surface.

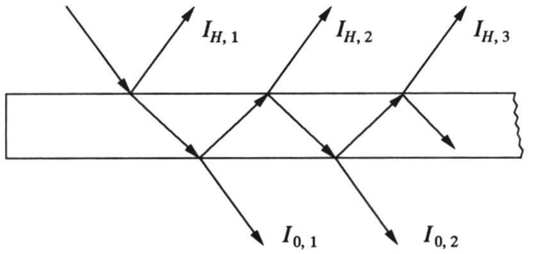

Fig. 8. Interpretation of diffraction process of neutrons by a non-absorbing thick crystal.

$$I_H^{(D)} = |R_{H,\infty}|^2 = \begin{cases} 1 & \text{for } |\eta| \le 1 \\ [|\eta| - (\eta^2 - 1)^{1/2}]^2 & \text{for } |\eta| \ge 1 \ . \end{cases} \qquad (3.2)$$

The profiles of the two rocking curves given by eqs.(3.1) and (3.2) differ considerably in their tail parts, and the Ewald formula gives twice the value of the Darwin formula at their far tails. Although experiments on the rocking curve have already been carried out,[20,21,28-31] relationship of the Ewald formula with the Darwin formula has been seldom studied.

The Ewald formula is usually obtained from the rocking curve which gives intensity from a finite crystal by taking the average over oscillations on the crystal thickness.[17,20,21] It is noted that this procedure is valid only when the reflected waves at the front and rear surfaces overlap coherently. However, this condition is broken in the ordinary experimental situation where the crystal thickness is much larger than the coherence length of neutrons.

Then the diffraction process should be explained by successive reflections at the front and rear surfaces as illustrated in Fig. 8.[32] The intensity of the transmitted beam through the rear surface $I_{0,1}$ is given by

$$I_{0,1} = (1 - I_{H,1})^2 \qquad (3.3)$$

in the case of non-absorbing crystals.[33] The beam reflected at the rear surface propagates toward the front surface, and the reflective intensity $I_{H,2}$ is given by

$$(1 - I_{H,1})^2 I_{H,1} \ . \qquad (3.4)$$

Thus the intensity of all the reflected beams is given by

$$I = \sum_{n=1}^{\infty} I_{H,n} = \frac{2I_{H,1}}{1+I_{H,1}} . \qquad (3.5)$$

The diffracted intensity $I_{H,1}$ should correspond to the Darwin formula $I_H^{(D)}$ given by eq.(3.2). Then one can show that eq.(3.5) is equivalent to the Ewald formula. Therefore a simple relation of

$$I_H^{(E)} = \frac{2I_H^{(D)}}{1+I_H^{(D)}} \qquad (3.6)$$

is obtained between the Darwin and Ewald formulae.

Similarly, the intensity of all the transmitted beams is given by

$$I = \sum_{n=1}^{\infty} I_{0,n} = \frac{1-I_H^{(D)}}{1+I_H^{(D)}} \qquad (3.7)$$

Experiments to test these relations were done at the beam-line C1-3 (ULS) in JRR-3M constructed for experiments on ultra-small angle neutron scattering and neutron optics. The double-crystal parallel setting of 111 reflection of Si crystals was used with the wavelength of 4.73Å. A channel-cut Si crystal using five successive reflections was adopted as the first crystal to reduce extremely the tail part of the incident beam on the second crystal.

The experiments were performed using two sample crystals with thicknesses of 10 mm and 1.4 mm, much larger than the coherence length. The first experiment was done using the crystal of 10 mm thickness. A slit was placed behind the sample crystal so that only the reflected beam $I_{H,1}$ is detected by a ^{3}He detector. In the second experiment, the crystal of 1.4 mm thickness was used and the slit was removed so as to detect significant parts of all the reflected beams $I_{H,n}$. The experimental result is shown in Fig. 9. Solid and broken curves were calculated based on eq.(3.2) and eq.(3.6), respectively, with the convolution of the reflectivity curve of the first crystal, $I_H^{(D)5}$. The experimental results agree well with the calculated ones.

The intensity of the transmitted beam has been also measured. Fig. 10 shows the intensity of all the forward diffracted beams in the case of the crystal of 1.4 mm thickness. The broken line was calculated by eq.(3.7). For comparison, the intensity of $1-I_{H,1}$ is shown by the solid line.

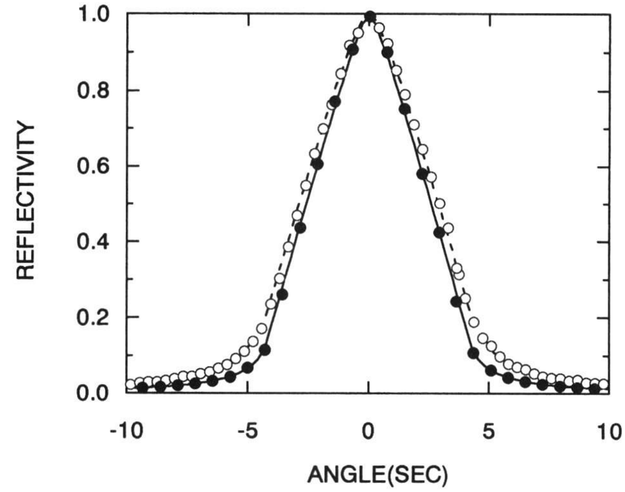

Fig. 9. Neutron rocking curves as a function of incident angle. Solid circles mean the reflectivity of a 10 mm thick crystal with a slit installed. Open circles represent the reflectivity of a 1.4 mm thick crystal while the slit was removed. Solid and broken curves were calculated based on eqs.(3.2) and (3.1), respectively.

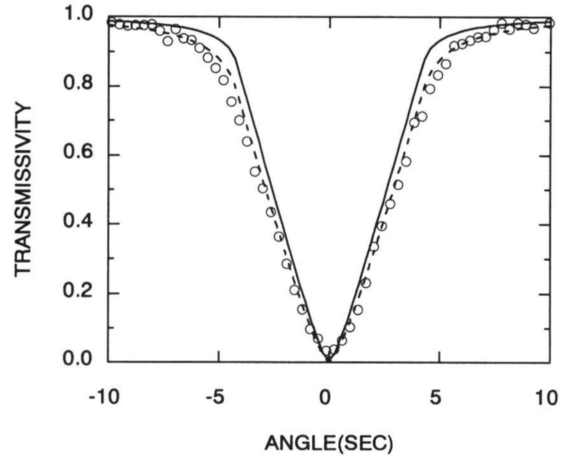

Fig. 10. Neutron rocking curve of the transmitted beam in the Bragg-case for a crystal with 1.4 mm thickness.

§.4. Proposed Test of Double Stern-Gerlach Experiments

Neutron interferometers made of Si crystals have been used to various kinds of experiments.[20,21,34] In particular they are suited for investigating the measurement theory in quantum mechanics. For instance, an experimental proposal on a double Stern-Gerlach experiment[35,36] has been done to test the superiority of measurement theories such as the many Hilbert theory[35] and the environment theory.[37] An experimental test has been proposed by using an interferometer made of multilayers.[37]

Here we propose a new type of interferometer made of perfect Si crystal designed for the double Stern-Gerlach experiment, as shown in Fig. 11. It consists of five crystal plates, three plates of which in the center work as the LLL-interferometer and function as the controller of neutron polarization states when a magnetic phase shifter with an appropriate thickness is inserted due to the effect of magnetic double refraction.[39-41] Therefore a test experiment whether interference occurs or not when unpolarized neutrons are decomposed at the components of LLL crystals will be possible.

§.5. Summary

Based on a new dynamical theory, we showed some properties of the reflectivity curve in the symmetric geometry, the Bragg diffraction of $\theta_B \cong 90°$, and the Fresnel reflectivity curve. We also showed a simple relation between the Ewald formula and the Darwin formula in the case of non-absorbing crystals. A test on the double Stern-Gerlach experiment was proposed.

1) S. Takagi, *Acta Cryst.* 15 (1962) 1131.
2) D. Taupin, *Bull. Soc. Fr. Mine'ral. Cristallogr.* 87 (1964) 469.
3) M.A.G. Halliwell, M.H. Lyons and M.J. Mill, *J. Cryst. Growth* 68 (1984) 523.
4) L.G. Parratt, *Phys. Rev.* 95 (1954) 359.
5) L. Névot and P. Croce, *Rev. Phys. Appl.* 15 (1980) 761.
6) T.P. Russell, *Mater. Sci. Rept.* 5 (1990) 171.
7) J. Penfold and R. K. Thomas, *J. Phys. Condens. Matter* 2 (1990) 1369.
8) I.K. Robinson, *Phys. Rev.* B 33 (1986) 3830.
9) R. Feidenhans'l, *Surf. Sci. Rep.* 10 (1989) 105.
10) I.K. Robinson, *Handbook on Synchrotron radiation* Vol. 3, eds. G. Brown and D.E. Moncton, (Elsevier, 1991), 221.
11) S. Nakatani and T. Takahashi, *Surf. Sci.* 311 (1994) 433.
12) T. Takahashi and S. Nakatani, *Surf. Sci.* 326 (1995) 347.
13) C.G. Darwin, *Phil. Mag.* 27 (1914) 675.
14) F. Abelés, *Ann. Phys.* 5 (1950) 706.
15) R.T. Perkins and L.V. Knight, *Acta Cryst.* A 40 (1984) 617.
16) M. von Laue, *Röntgenstrahl-Interferenzen* (Akademische Verlag, Frankfurt, 1960).
17) W.H. Zachariasen, *Theory of X-Ray Diffraction in Crystals* (Dover, New York, 1945).
18) B.W. Batterman and H. Cole, *Rev. Mod. Phys.* 36 (1964) 681.
19) N. Kato, *X-Ray Diffraction,* Ed. L.V. Azároff (McGraw-Hill, 1974), p.222.
20) H. Rauch and D. Petrascheck, *Neutron Diffraction,* Ed. H. Dachs, Topics in Current Physics Vol. 6 (Springer-Verlag, Berlin, 1978), p.303.
21) V.F. Sears, *Neutron Optics* (Oxford Univ. Press, 1989).
22) K. Kohra and T. Matsushita, *Z. Naturforsch.* 27a (1972) 484.
23) O. Brümmer, H.R. Hōche and J. Nieber, *Phys. Stat. Sol.* (a) 53 (1979) 565.
24) A. Caticha and S. Caticha-Ellis, *Phys. Rev.* B 25(1982) 971.
25) T. Ohta, Y. Kitajima, H. Kuroda, T. Takahashi and S. Kikuta, *Nucl. Instrum. Meth.* A246 (1986) 760.
26) D.P. Woodruff, D.L. Seymour, C.F. McConville, C.E. Riley, M.D. Crapper, N.P. Prince and R.G. Jones, *Surf. Sci.* 195 (1988) 237.
27) P.P. Ewald, *Ann. Physik* (Leipzig) 54 (1917) 557.
28) S.G. Shull, *J. Appl. Cryst.* 6 (1973) 257.
29) S. Kikuta, I. Ishikawa, K. Kohra and S. Hoshino, *J. Phys. Soc. Jpn* 39 (1975) 471.
30) S. Kikuta, T. Takahashi, K. Nakayama, Y. Fujii and S. Hoshino, *J. Phys. Soc. Jpn* 45 (1978) 1065.
31) W. Treimer, W. Fielder and B. Bükert, *Phys. Lett.* 110A (1985) 173.
32) T. Takahashi and M. Hashimoto, *Phys. Lett.* A 200 (1995) 73.
33) U. Bonse and M. Hart, *Z. Physik* 194 (1966) 1.
34) A.G. Klein and S.A. Werner, *Rep. Prog. Phys.* 46 (1983) 259.
35) S. Machida and M. Namiki, *Prog. Theor. Phys.* 63 (1980) 1457, 1833.
36) S. Machida and M. Namiki, *Proceedings of the 2nd International Symposium on Foundations Quantum Mechanics* (ISQM-Tokyo 86), ed. M. Namiki et al. (Physical Society of Japan, 1987), 355.
37) W.H. Zurek, *Phys. Rev.* D 24 (1981) 1516.
38) T. Ebisawa, S. Tasaki, Y. Otake and H. Funahashi, *Physica* B 213/214 (1995) 957.
39) S. Nakatani, Y. Hasegawa, H. Tomimitsu, T. Takahashi and S. Kikuta, Jpn. *J. Appl. Phys.* 30 (1991) L867.
40) S. Nakatani, H. Tomimitsu, T. Takahashi and S. Kikuta, *Jpn. J. Appl. Phys.* 31 (1992) L1137.
41) S. Nakatani, H. Tomimitsu, T. Takahashi and S. Kikuta, in this workshop.

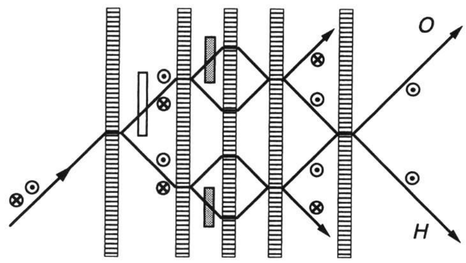

Fig. 11. A new type of interferometer made of five crystal plates for the double Stern-Gerlach experiment. Magnetic phase shifters (hatched) are inserted to decompose neutron spins.